Predictive analysis of water wettability and corrosion resistance of secondary AlSi10MnMg(Fe) alloy manufactured by vacuum assisted high pressure die casting

UNIVERSITY of WISCONSIN
UWMILWAUKEE

Swaroop K. Behera[1], Amir Kordijazi[2], Arthur Jamet[3], Ana Isabel Fernández-Calvo[4], Pradeep Rohatgi[1]

[1]Department of Materials Science and Engineering, University of Wisconsin Milwaukee, 53211 USA
[2]Department of Industrial and Manufacturing Engineering, University of Wisconsin Milwaukee, 53211 USA
[3]Department of Mechanical Engineering, University of Nantes, 44035 France
[4]AZTERLAN, Basque Research and Technology Alliance (BRTA), Aliendalde Auzunea 6, 48200-Durango, Spain

INTRODUCTION

- Secondary Aluminum alloys are lucrative for the automotive industry; however, they have reduced ductility due to the formation of detrimental β intermetallics.
- A modified secondary aluminum alloy ($AlSi_{10}MnMg(Fe)$) was developed to reduce the formation of these intermetallics.
- The focus of the current work is to study and predict the effect of Mn addition, and cooling rate in vacuum-assisted HPDC on water wettability of secondary $AlSi_{10}MnMg(Fe)$.
- Since wettability influences corrosion resistance of cast alloys, these studies would enable prediction of corrosion resistance as well.
- A data driven approach is useful in predicting the wetting behavior as theoretical modelling of these surfaces and wetting characteristics leaves further possibilities of interactions.

EXPERIMENTAL METHOD

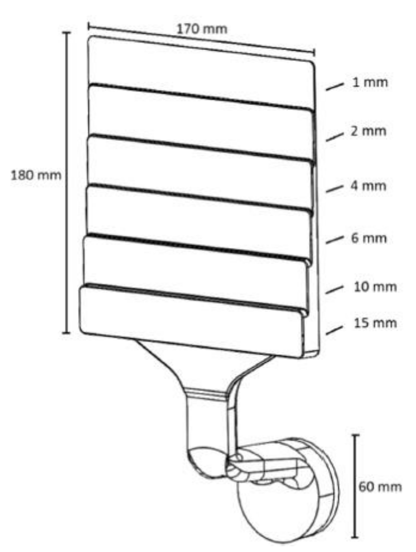

- **Microscopy** (Optical and SEM) – Phase determination
- Confocal Microscopy - Roughness Measurements
- **Goniometer** – Contact Angle measurements
- **Linear polarization** – Corrosion rate measurements
- **Neural Network Model** – Data prediction

Figure 1. Design of the step cast test part

Alloy*	Si	Fe	Mn	Mg	Cu	Zn	Ti	Sr
E - Primary	10.70	0.17	0.68	0.47	<0.01	0.01	0.05	0.006
C - Secondary	9.92	0.62	0.42	0.37	0.04	0.03	0.04	0.005

Table 1. Composition of the two alloys used in this study

Factor	Type	Levels	Values
Section size (mm)	Fixed	5	1, 4, 6, 10, 15
Droplet size (µL)	Fixed	2	2, 4
Alloy Type (Primary or secondary)	Fixed	2	C, E

Table 2. Independent Factors And Their Levels

ANN Architecture (Figure 3)

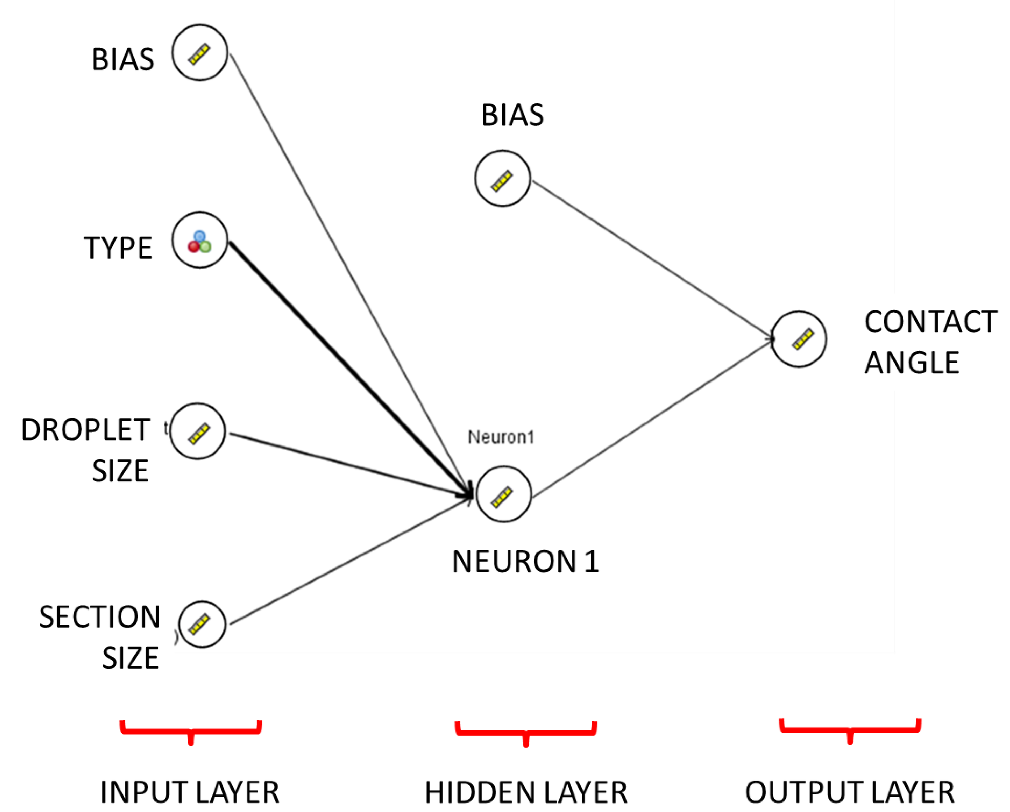

- From our previous studies, the contact angle values of Al-Si alloys do not follow a linear relationship with the independent factors.
- Therefore, in this study, an Artificial Neural Network (ANN) model was developed.
- ANN is a predictive model representing simple mathematical models of the brain.
- It can be applied to model complex nonlinear relationships between the response variable and its predictors.

RESULTS

ANN Model - Accuracy

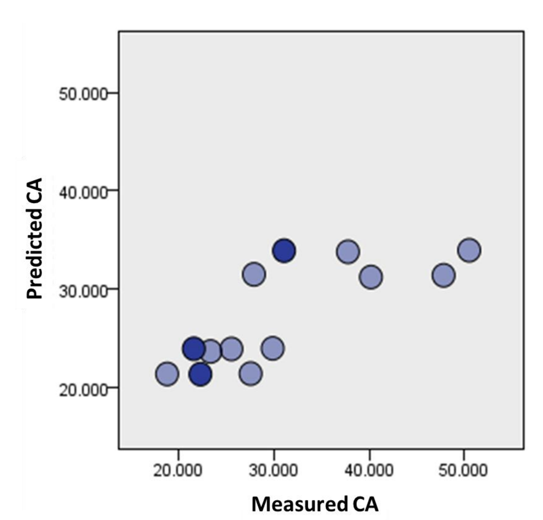

Table 3. Error And R-Square Of The ANN Model For Each Partition

'Partition'	Training	Testing
Minimum Error	-3.878	-6.095
Maximum Error	16.557	1.125
Mean Error	2.798	-2.873
Mean Absolute Error	4.897	3.435
Standard Deviation	6.555	3.102
Linear Correlation	0.755	0.874
Occurrences	16	4

Figure 4. Scatter plot of predicted values vs. measured values of CA

ANN Model - Robustness

Table 4. Error And R-Square Of The Developed ANN Model In Prediction Of The Outcome Of New Input Data

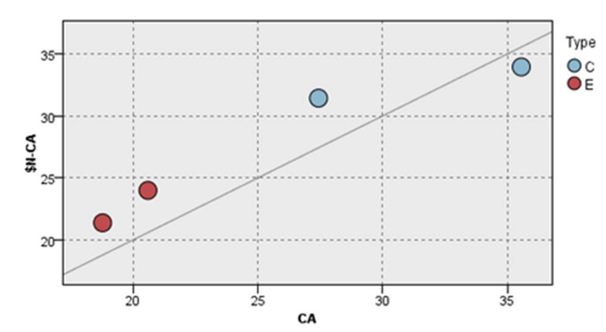

Partition	Testing
Minimum Error	-4.003
Maximum Error	1.603
Mean Error	-2.098
Mean Absolute Error	2.899
Standard Deviation	2.533
Linear Correlation	0.959
Occurrences	4

Figure 5. Scatter plot for predicted values and observed values for 2mm step

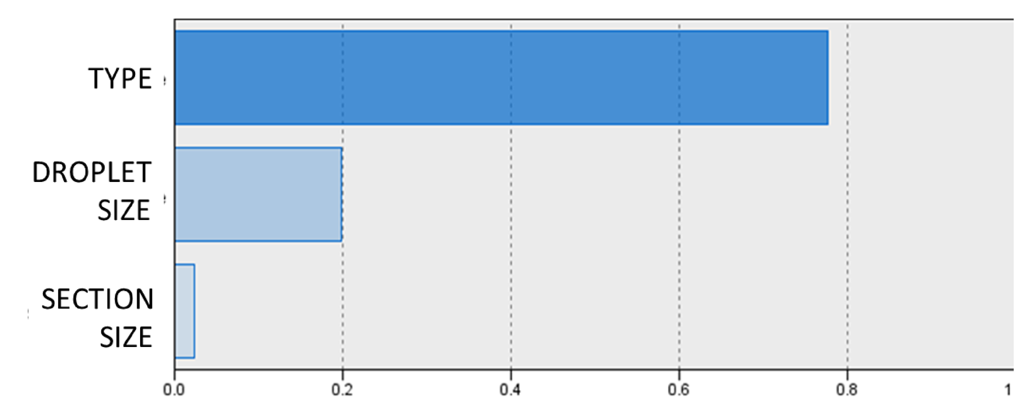

Figure 6. Importance of each predictor in the outcome

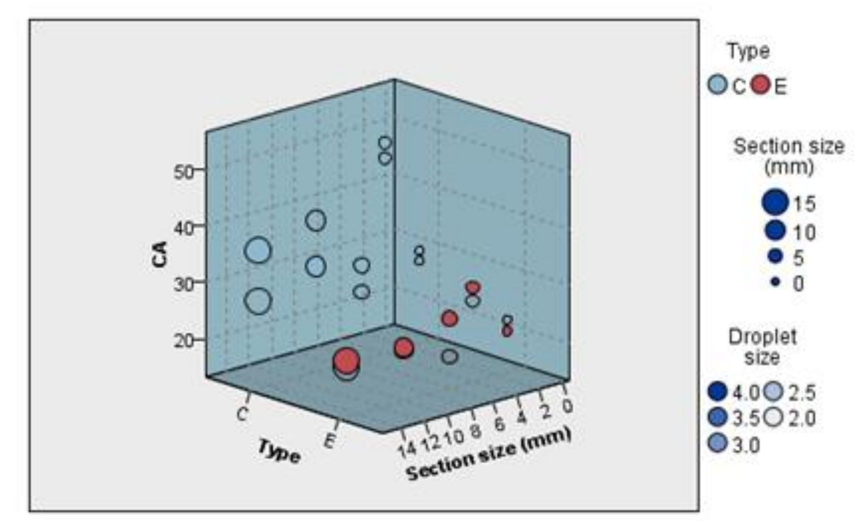

Figure 7. 3D plot of CA values vs. predictor variables

Effect of microstructure

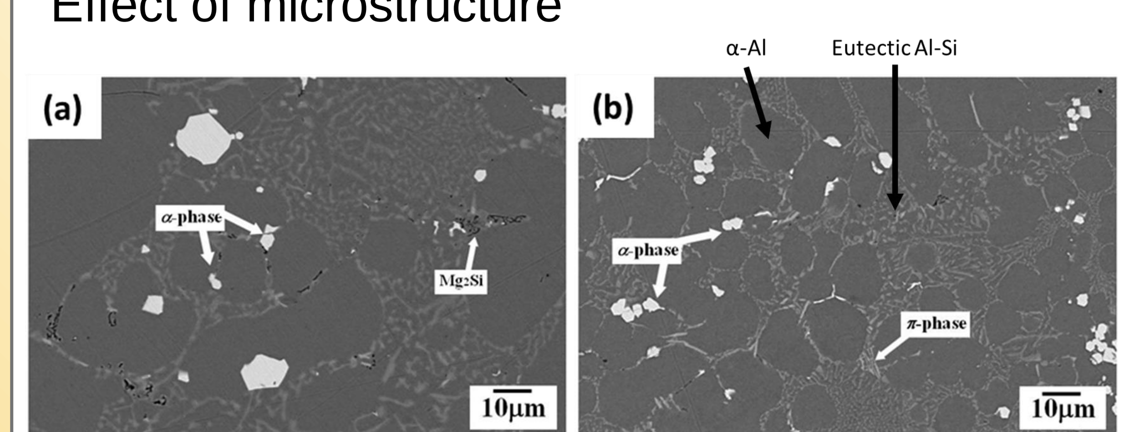

Figure 8. SEM micrographs showing the presence of intermetallic compounds in the two alloys in 10 mm step (a) primary alloy E and (b) secondary alloy C

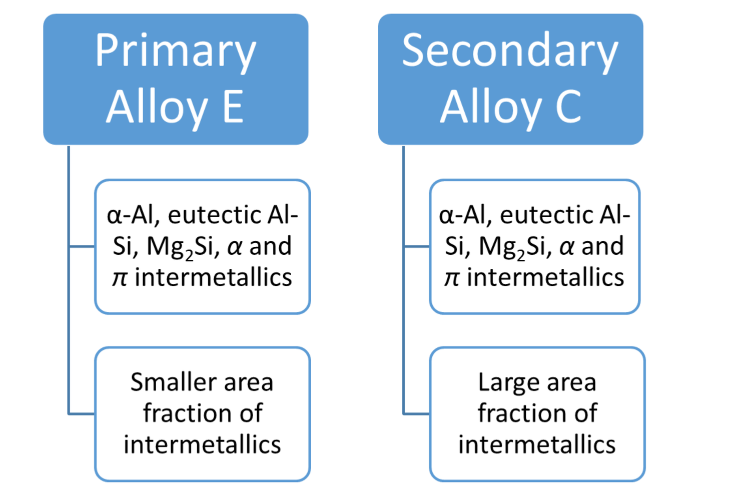

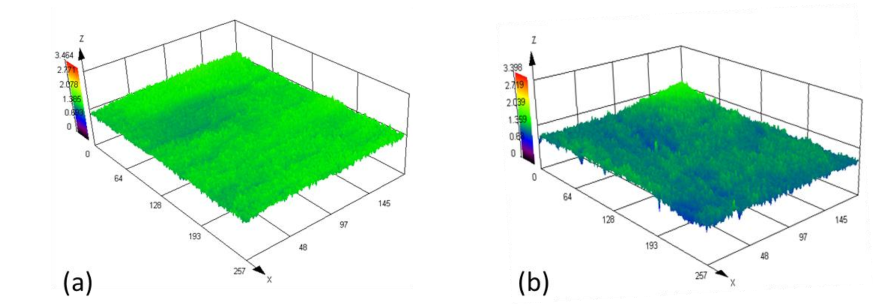

Figure 9. Confocal images of primary and secondary alloys

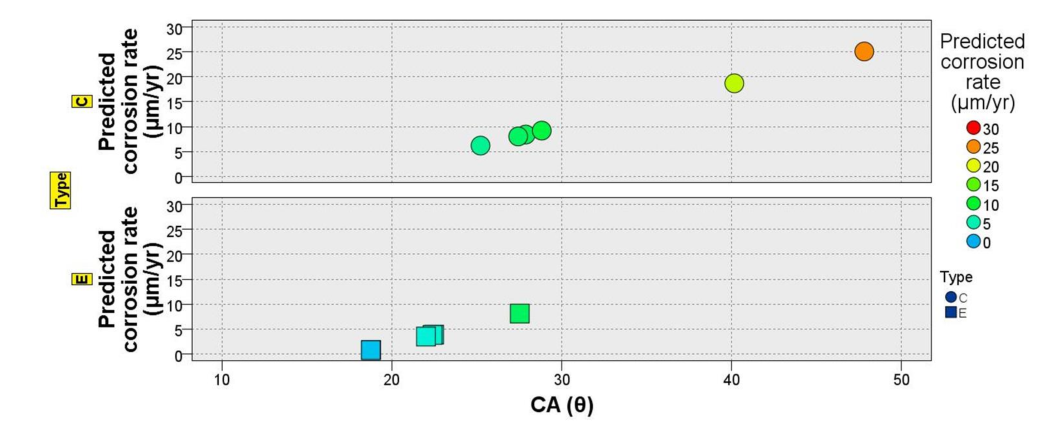

Figure 10. Scatter plot of predicted corrosion rate (µm) vs. contact angle for the primary (bottom plot) and secondary (top plot) alloys with different cooling rate

CONCLUSIONS

- The water wettability and corrosion resistance of primary and secondary $AlSi_{10}MnMg(Fe)$ alloys were studied as a function of the physical and chemical properties of the surface.
- **Artificial Neural Network** - to map the input data (**alloy type**, **droplet size**, **section size**) to the output (CA).
- **Developed ANN model** – able to predict unseen CA values with high accuracy (r = 0.96).
- **Topographical and microscopy images** - Large intermetallic phase fraction = higher heterogeneity = high surface roughness = greater CA values
- **Corrosion Studies** - **primary alloy** is more corrosion resistant than the **secondary alloy** due to the less galvanic sites. Additionally, increasing surface roughness = reduced corrosion resistance.
- These findings can be used as a guide to design and optimize surface composition, structure and roughness to improve corrosion resistance of cast secondary aluminum alloys.

References

1.Niklas, A., Bakedano, A., Orden, S., da Silva, M., Nogués, E., and Fernández-Calvo, A.I. (2015). Effect of Microstructure and Casting Defects on the Mechanical Properties of Secondary AlSi10MnMg(Fe) Test Parts Manufactured by Vacuum Assisted high Pressure Die Casting Technology. Materials Today: Proceedings *2*, 4931–4938.
2.Niu, X.P., Hu, B.H., Pinwill, I., and Li, H. (2000). Vacuum assisted high pressure die casting of aluminium alloys. Journal of Materials Processing Technology *105*, 119–127.
3.Vinarcik, E.J. (2002). High integrity die casting processes (John Wiley & Sons).
4.Shankar, S., and Apelian, D. (2002). Die soldering: Mechanism of the interface reaction between molten aluminum alloy and tool steel. Metallurgical and Materials Transactions B *33*, 465–476.
5.Shabestari, S.G. (2004). The effect of iron and manganese on the formation of intermetallic compounds in aluminum–silicon alloys. Materials Science and Engineering: A *383*, 289–298.
6.Shankar, S. (2002). A study of the interface reaction mechanism between molten aluminum and ferrous die materials.
7.Niklas, A., Fernández-Calvo, A.I., Bakedano, A., Orden, S., da Silva, M., Nogués, E., and Roset, E. (2016). A new secondary AlSi10MnMg (Fe) Alloy suitable for manufacturing of ductile Aluminium parts by vacuum assisted high pressure die casting technology. METALLURGIA ITALIANA, 17–20.
8.Niklas, A., Orden, S., Bakedano, A., Da Silva, M., Nogués, E., and Fernández-Calvo, A.I. (2016). Effect of solution heat treatment on gas porosity and mechanical properties in a die cast step test part manufactured with a new AlSi10MnMg (Fe) secondary alloy. Materials Science and Engineering: A *667*, 376–382.
9.Kucharikova, L., Tillová, E., Chalupová, M., Mazur, M., Herčko, A., and Čička, R. (2019). Analysis of microstructure in AlSi7Mg0.3 cast alloy with different content of Fe. Transportation Research Procedia *40*, 59–67.
10.Ramachandran, R., and Nosonovsky, M. (2015). Coupling of surface energy with electric potential makes superhydrophobic surfaces corrosion-resistant. Physical Chemistry Chemical Physics *17*, 24988–24997.
11.Liang, J., Hu, Y., Wu, Y., and Chen, H. (2014). Facile formation of superhydrophobic silica-based surface on aluminum substrate with tetraethylorthosilicate and vinyltriethoxysilane as co-precursor and its corrosion resistant performance in corrosive NaCl aqueous solution. Surface and Coatings Technology *240*, 145–153.
12.Liu, T., Dong, L., Liu, T., and Yin, Y. (2010). Investigations on reducing microbiologically-influenced corrosion of aluminum by using super-hydrophobic surfaces. Electrochimica Acta *55*, 5281–5285.
13.Bhushan, B. (2013). Introduction to tribology (John Wiley & Sons).
14.Nosonovsky, M., and Bhushan, B. (2012). Green tribology: biomimetics, energy conservation and sustainability (Springer).
15.Young Thomas (1805). III. An essay on the cohesion of fluids. Philosophical Transactions of the Royal Society of London *95*, 65–87.
16.Hejazi, V. (2014). Wetting, superhydrophobicity, and icephobicity in biomimetic composite materials.
17.Kwok, D.Y., Lam, C.N.C., Li, A., Leung, A., Wu, R., Mok, E., and Neumann, A.W. (1998). Measuring and interpreting contact angles: a complex issue. Colloids and Surfaces A: Physicochemical and Engineering Aspects *142*, 219–235.
18.Lam, C.N.C., Wu, R., Li, D., Hair, M.L., and Neumann, A.W. (2002). Study of the advancing and receding contact angles: liquid sorption as a cause of contact angle hysteresis. Advances in Colloid and Interface Science *96*, 169–191.
19.Tavana, H., Lam, C.N.C., Grundke, K., Friedel, P., Kwok, D.Y., Hair, M.L., and Neumann, A.W. (2004). Contact angle measurements with liquids consisting of bulky molecules. Journal of Colloid and Interface Science *279*, 493–502.
20.Chau, T.T. (2009). A review of techniques for measurement of contact angles and their applicability on mineral surfaces. Minerals Engineering *22*, 213–219.
21.Kordijazi, A., Behera, S.K., Akbarzadeh, O., Povolo, M., and Rohatgi, P. (2020). A Statistical Analysis to Study the Effect of Silicon Content, Surface Roughness, Droplet Size and Elapsed Time on Wettability of Hypoeutectic Cast Aluminum–Silicon Alloys. In Light Metals 2020 (Springer), pp. 185–193.
22.Kordijazi, A., Kumar Behera, S., Suri, S., Wang, Z., Povolo, M., Salowitz, N., and Rohatgi, P. (2020). Data-Driven Modeling of Wetting Angle and Corrosion Resistance of Hypereutectic Cast Aluminum-Silicon Alloys Based on Physical and Chemical Properties of Surface. Surfaces and Interfaces, 100549.
23.Kordijazi, A., Roshan, H.M., Dhingra, A., Povolo, M., Rohatgi, P.K., and Nosonovsky, M. (2020). Machine-learning methods to predict the wetting properties of iron-based composites. Surface Innovations, 1–9.
24.Kordijazi, A., Weiss, D., Das, S., Behera, S., Roshan, H.M., and Rohatgi, P. Effect of Solidification Time on Microstructure, Wettability, and Corrosion Properties of A205-T7 Aluminum Alloys. International Journal of Metalcasting, 1–11.
25.Das, S., Kordijazi, A., Akbarzadeh, O., and Rohatgi, P.K. An innovative process for dispersion of graphene nanoparticles and nickel spheres in A356 alloy using pressure infiltration technique. Engineering Reports, e12110.
26.Montgomery, D.C., and Runger, G.C. (2010). Applied statistics and probability for engineers (John Wiley & Sons).
27.Cassie, A.B.D., and Baxter, S. (1944). Wettability of porous surfaces. Transactions of the Faraday society *40*, 546–551.
28.Wenzel, R.N. (1936). Resistance of solid surfaces to wetting by water. Industrial & Engineering Chemistry *28*, 988–994.
29.Vafaei, S., and Podowski, M.Z. (2005). Theoretical analysis on the effect of liquid droplet geometry on contact angle. Nuclear Engineering and Design *235*, 1293–1301.
30.ASTM, G. (2004). Standard practice for calculation of corrosion rates and related information from electrochemical measurements. G102-89, ASTM International, West Conshohocken, USA.
31.Birbilis, N., and Buchheit, R.G. (2005). Electrochemical characteristics of intermetallic phases in aluminum alloys an experimental survey and discussion. Journal of The Electrochemical Society *152*, B140–B151.
32.Li, J., and Dang, J. (2017). A Summary of Corrosion Properties of Al-Rich Solid Solution and Secondary Phase Particles in Al Alloys. Metals *7*, 84.
33.Ahn, C., and Lee, E. (2019). [ICACE2019] Effect of cooling rate on the corrosion resistance and mechanical property of AlSi 10 MnMg alloy. 한국마린엔지니어링학회지 *43*, 618–624.
34.Berlanga, C., Bakedano, A., de Ciriza, A.P., Rivero, P.J., Mendez, S., Rodriguez, R., and Niklas, A. (2019). Evaluation of the corrosion resistance of a new AlSi10MnMg (Fe) secondary alloy. Materials Today: Proceedings *10*, 312–318.
35.Kordijazi, A. (2019). Optimization of Ni–P–Zn electroless bath and investigation of corrosion resistance of as-plated coatings. Materials Research Express *6*, 096565.
36.Almansour, A., Azizi, M., Jesri, A.M., and Entakly, S. (2015). Effect of surface roughness on corrosion behavior of aluminum alloy 6061 in salt solution (3.5% NaCl). International Journal of Academic Scientific Research *3*, 37–45.